Dalton Transactions

ROYAL SOCIETY OF CHEMISTRY

COMMUNICATION

View Article Online
View Journal | View Issue

Cite this: *Dalton Trans.*, 2025, **54**, 17425

Received 8th August 2025,
Accepted 30th October 2025

DOI: 10.1039/d5dt01893e

rsc.li/dalton

A disilane-bonded bis(methylpyridine) Cu(I) complex exhibiting reversible trigonal–tetrahedral switch with stimuli-responsive luminescence

Yoshinori Yamanoi, *[a] Yongjin Zhao,[b] Toyotaka Nakae,[a] Kaito Segawa,[c,d] Masaki Yoshida,[c,e] Masako Kato,[c] Kazuma Kikuchi,[f] Hiroaki Imoto,[f] Kensuke Naka,[f] Showa Kitajima,[g] Hitoshi Kasai,[g] Kouki Oka[g] and Suguru Ito *[b]

A stimuli-responsive tetranuclear copper(I) complex with 1,1,2,2-tetramethyl-1,2-bis(3-methylpyridin-2-yl)disilane (L1) showed reversible structural transformation between $Cu_4I_4(L1)_2{\cdot}2CH_3CN$ and $Cu_4I_4(L1)_2$. The change altered copper coordination from a tetrahedral to trigonal type as confirmed by XRD. The solvated form showed stronger blue-green emission (λ_{em} = 493 nm, Φ = 0.56) than the desolvated form (λ_{em} = 471 nm, Φ = 0.06). The change in emission intensity in the crystalline state was attributed to the change in structural rigidity or flexibility induced by the coordination or non-coordination of CH_3CN to the Cu(I) center.

Luminescent materials have attracted significant attention over the past decades due to their wide range of applications as smart materials.[1] Among them, stimuli-responsive luminescent metal complexes have emerged as a research hotspot in recent years, owing to the structural modification of organic ligands and the high stability.[2] In particular, copper(I) complexes are promising candidates for available crystalline-state emitters due to their diverse structural motifs and occasionally observed polymorphs.[3] Extended π-conjugated ligands are commonly employed to construct the functional copper(I) complexes.

We have previously investigated stimuli-responsive σ–π conjugated aromatic disilane molecules,[4] and reported crystalline polymorphs of copper(I) iodide complexes with 1,1,2,2-tetramethyl-1,2-di(pyridin-2-yl)disilane (**L**), which form an octanuclear complex at room temperature and a one-dimensional polymer at 77 K *via* a single-crystal-to-single-crystal phase transition.[5] Additionally, we reported the optical properties of trigonal planar mononuclear Cu(I) complexes bearing disilane-bonded bis(methylpyridine) ligands.[6–8] These complexes exhibited intense emission in the crystalline state and aggregation-induced emission (AIE) in THF–water mixtures.

Vapochromic luminescence of copper(I) complexes has been widely investigated.[9] In many reported systems, the change in the emission colour in the crystalline state is due to the reversible exchange of different solvent molecules at the metal center.[10] However, these changes are typically attributed to electronic effects rather than structural changes. In contrast, only a limited number of studies have addressed the direct impact of solvent coordination/uncoordination on the metal centre geometry, which can significantly affect emission behaviour.[11] Coordination of solvent molecules to the metal ion generally induces structural distortions and activates high-energy vibrational modes associated with C–H bonds, which promote non-radiative decay pathways resulting in decreased emission intensity in the crystalline state.[12]

In this study, we investigated the reversible structural transformation (Fig. 1b) and luminescence changes in a tetranuclear copper(I) iodide complex synthesized using a flexible ligand **L1** (Fig. 1a), in which a methyl group is introduced into the pyridine rings. We found that exposure to CH_3CN vapor triggers coordination to the copper centres, transforming the flexible trigonal geometry into a more rigid tetrahedral arrangement. This structural change led to a significant enhancement in both luminescence efficiency and lifetime. These findings provide new insights into the relationship between the molecular structure and photophysical properties in the crystalline state and offer a novel strategy for designing stimuli-responsive luminescent materials.

[a]*Department of Chemistry, School of Science, The University of Tokyo, 7-3-1 Hongo, Bunkyo-ku, Tokyo 113-0033, Japan. E-mail: ymanoi@chem.s.u-tokyo.ac.jp*
[b]*Department of Chemistry and Life Science, Graduate School of Engineering Science, Yokohama National University, Yokohama, Kanagawa 240-8501, Japan. E-mail: suguru-ito@ynu.ac.jp*
[c]*Department of Applied Chemistry for Environment, School of Biological and Environmental Sciences, Kwansei Gakuin University, 1 Gakuen Uegahara, Sanda, Hyogo 669-1330, Japan*
[d]*Department of Chemistry, Faculty of Science, Kyushu University, 744 Motooka, Nishi-ku, Fukuoka 819-0395, Japan*
[e]*Department of Chemistry, Graduate School of Science, The University of Osaka, 1-1 Machikaneyama, Toyonaka, Osaka 560-0043, Japan*
[f]*Faculty of Molecular Chemistry and Engineering, Graduate School of Science and Technology, Kyoto Institute of Technology, Goshokaido-cho, Matsugasaki, Sakyo-ku, Kyoto 606-8585, Japan*
[g]*Institute of Multidisciplinary Research for Advanced Materials, Tohoku University, Sendai, Miyagi 980-8577, Japan*

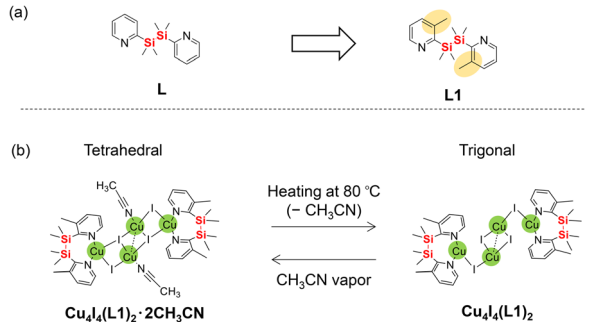

Fig. 1 (a) Chemical structures of disilane-bonded **L** (previous work) and **L1** (this work). (b) Chemical structures of stimuli-responsive copper complexes in this work.

The tetrahedral copper(I) complex **$Cu_4I_4(L1)_2{\cdot}2CH_3CN$** was synthesized by mixing CuI and **L1** in a 2 : 1 molar ratio in CH_3CN at room temperature (Scheme 1a). The complex was isolated as air-stable crystals in 24% yield. The acetonitrile-free complex **$Cu_4I_4(L1)_2$** was quantitatively obtained by heating **$Cu_4I_4(L1)_2{\cdot}2CH_3CN$** at 80 °C (Scheme 1b).

The structures of both complexes were confirmed by single-crystal X-ray diffraction.[13] The molecular structure of **$Cu_4I_4(L1)_2{\cdot}2CH_3CN$** is shown in Fig. 2a. The complex adopts a Cu_4I_4 core with distorted tetrahedral coordination geometries, in which acetonitrile molecules are coordinated to the copper centres. The iodide ligands exhibit both μ_2- and μ_3-bridging modes. The Cu6–N9 distance between CH_3CN and Cu(I) is 2.015 Å,[14] suggesting a relatively weak interaction and implying that CH_3CN can be easily removed upon external stimuli.

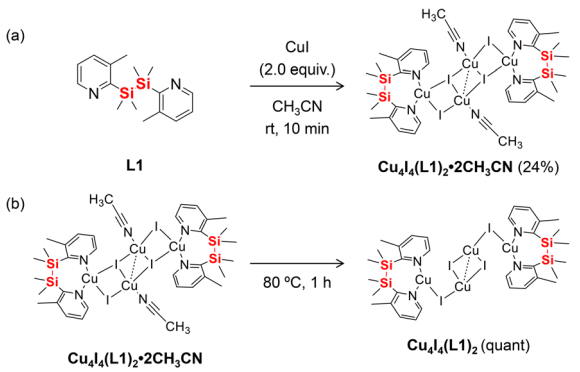

Scheme 1 Synthetic scheme of **$Cu_4I_4(L1)_2{\cdot}2CH_3CN$** and **$Cu_4I_4(L1)_2$**.

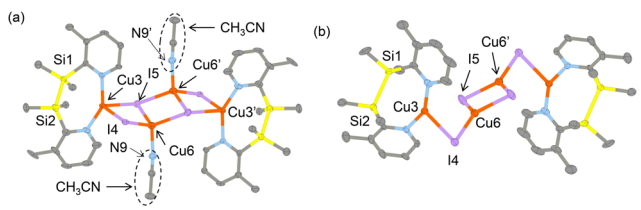

Fig. 2 X-ray structures of (a) **$Cu_4I_4(L1)_2{\cdot}2CH_3CN$** and (b) **$Cu_4I_4(L1)_2$** with thermal ellipsoids with 50% probability. Hydrogen atoms are omitted for clarity.

The coordination environment around Cu3 and Cu3′ is significantly distorted from the ideal tetrahedral geometry, while Cu6 and Cu6′ adopt nearly regular tetrahedral geometries. The Cu6–Cu6′ distance is 2.850 Å, which closely matches twice the covalent radius of copper (1.32 Å), indicating the presence of intramolecular Cu(I)···Cu(I) cuprophilic interactions.[15] In contrast, the Cu3–Cu6 distance is 3.4019 Å, suggesting no significant metal–metal interaction. The crystal packing (Fig. S1a) is stabilized by C≡N···π, C–H···π, and non-classical I···H–C hydrogen bonding interactions.[16]

The Cu–I distances were Cu3–I4 = 2.762 Å, Cu3–I5 = 2.949 Å, Cu6–I5 = 2.664 Å, and Cu6–I4 = 2.634 Å. The longer Cu3–I5 suggests that the linkage is readily cleaved upon CH_3CN dissociation, leading to the formation of a three-coordinate complex.

Bourissou and co-workers reported that disilane-bonded diphosphine ligands can exhibit σ(Si–Si) coordination to copper centers.[17] In their work, coordination of the Si–Si σ-bond to cationic Cu centres resulted in elongated Si–Si bonds (~2.45 Å, compared to ~2.36 Å in the free ligand) and Si–Cu bond lengths (~2.72 Å), slightly exceeding the sum of van der Waals radii (2.43 Å). In contrast, in **$Cu_4I_4(L1)_2{\cdot}2CH_3CN$**, the Si–Si bond length is 2.37 Å, close to that in the free ligand (*ca.* 2.33 Å), and the Si–Cu distance is 2.90 Å—significantly longer than the expected van der Waals contact. These results indicate that the disilane moiety in **L1** does not coordinate to the Cu(I) centres in this complex.

The bond angles around Cu3 (Cu3′) are: N8–Cu3–N7 = 144.12°, N8–Cu3–I4 = 106.07°, N7–Cu3–I4 = 102.38°, and I5–Cu3–I4 = 97.32°, consistent with a distorted tetrahedral geometry. The bond angles around Cu6 (Cu6′) are: N9–Cu6–I4 = 106.41°, I5–Cu6–I4 = 108.14°, I5–Cu6–I5′ = 115.09°, and N9–Cu6–I5′ = 111.35°, closely resembling an ideal tetrahedral structure.

Upon heating **$Cu_4I_4(L1)_2{\cdot}2CH_3CN$** at 80 °C for 1 h, the crystals transformed into the acetonitrile-free colourless complex **$Cu_4I_4(L1)_2$**. The crystal structure of this phase is shown in Fig. 2b. It crystallizes in the monoclinic system (space group $P\bar{1}$), and all Cu(I) centres adopt a trigonal planar geometry. The sum of bond angles around Cu3 (Cu3′) and Cu6 (Cu6′) are 358.72° and 359.99°, respectively, confirming near-planar coordination environments.

The Cu–I bond lengths are as follows: Cu3–I4 = 2.761 Å, Cu6–I4 = 2.535 Å, Cu6–I5 = 2.578 Å, and Cu6–I5′ = 2.541 Å. The Cu3–I5 (or Cu3′–I5′) distances are 3.602 Å, indicating negligible Cu···I interaction at these positions. The I–Cu–I bond angles are in the range of 97.3° to 115.1°. There is no significant Cu3–Cu6 interaction (3.001 Å), which exceeds the sum of van der Waals radii, while the Cu6–Cu6′ distance is 2.784 Å, shorter than that in **$Cu_4I_4(L1)_2{\cdot}2CH_3CN$**, indicating stronger cuprophilic interactions in **$Cu_4I_4(L1)_2$**.

No evidence of interaction between the Si–Si bond and the Cu(I) centres was observed in **$Cu_4I_4(L1)_2$** as well. The crystal packing of **$Cu_4I_4(L1)_2$** is stabilized by face-to-face CH···π inter-

actions between methylpyridine units and non-classical I···H–C hydrogen bonds (Fig. S1b).

To gain deeper insights into the polymorphic behaviour of **$Cu_4I_4(L1)_2$·2CH_3CN**, powder X-ray diffraction (PXRD) analysis was carried out. The results are shown in Fig. S3. Upon heating the crystalline sample at 80 °C, the PXRD pattern underwent a clear transformation, corresponding to the loss of coordinated CH_3CN and formation of **$Cu_4I_4(L1)_2$**. Remarkably, the original pattern of **$Cu_4I_4(L1)_2$·2CH_3CN** was restored upon exposure to CH_3CN vapor, indicating a reversible crystal-to-crystal phase transition. Simulated PXRD patterns based on single-crystal X-ray structures matched well with the experimental data for both phases, confirming the structural reversibility. Such reversible formation and cleavage of Cu–I bonds have also been observed in previous studies (copper(I) iodide complexes with 1,1,2,2-tetramethyl-1,2-di(pyridin-2-yl)disilane (**L**)) and represent an important example of the reversible stimulus-responsive behaviour of Cu(I) complexes.[5]

Thermogravimetric analysis (TGA) of **$Cu_4I_4(L1)_2$·2CH_3CN** (Fig. S2) further supported this transformation. A distinct weight loss of approximately 6% was observed at around 80 °C, corresponding to the loss of two CH_3CN molecules per **$Cu_4I_4(L1)_2$** unit. No additional weight loss occurred up to 180 °C, demonstrating the thermal stability of the **$Cu_4I_4(L1)_2$** complex. Decomposition of the framework commenced beyond 180 °C.

Most of the metal complexes that show vapochromic emission have been studied in terms of coordination between different vapor molecules. However, there are a few examples that have examined in detail the solvent coordination/non-coordination crystalline complexes.[18] In this study, a clear vapochromic response caused by the coordination and dissociation of CH_3CN was observed between **$Cu_4I_4(L1)_2$·2CH_3CN** and **$Cu_4I_4(L1)_2$** in the crystalline state. As shown in Fig. 3, **$Cu_4I_4(L1)_2$·2CH_3CN** forms yellow-green cubic crystals under ambient light and displays green emission under UV irradiation. Upon heating to 80 °C, the coordinated CH_3CN molecules are released, resulting in desolvated **$Cu_4I_4(L1)_2$** crystals, which are colourless under ambient light and emit blue luminescence under UV light. The emission maxima were 493 nm for **$Cu_4I_4(L1)_2$·2CH_3CN** and 471 nm for **$Cu_4I_4(L1)_2$**, respectively. Exposure of the desolvated crystals to CH_3CN vapor led to rapid recovery of the original emission and colour, indicating a reversible crystal-to-crystal phase transition mediated by CH_3CN coordination. This process could be repeated multiple times without degradation.

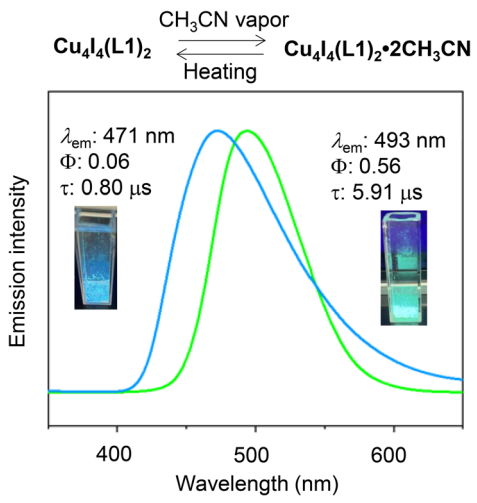

Fig. 3 Photographs showing the emission colour under UV (365 nm) irradiation and emission spectra with excitation at 370 nm between **$Cu_4I_4(L1)_2$·2CH_3CN** and **$Cu_4I_4(L1)_2$** in the crystalline state under external stimuli.

Photoluminescence quantum yield (PLQY) and emission lifetime measurements further highlight the significant effect of CH_3CN coordination. **$Cu_4I_4(L1)_2$·2CH_3CN** exhibited a PLQY of 0.56 and an emission lifetime of 5.91 μs, while **$Cu_4I_4(L1)_2$** displayed a much lower PLQY of 0.06 and a shorter lifetime of 0.80 μs. The higher PLQY and longer emission lifetime of **$Cu_4I_4(L1)_2$·2CH_3CN** are attributed to the enhanced radiative rate (k_r) and reduced non-radiative rate (k_{nr}) resulting from the rigid structure (Table S2).[19]

Next, the emission behaviour of **$Cu_4I_4(L1)_2$** and **$Cu_4I_4(L1)_2$·2CH_3CN** was investigated at 77 K (Tables S1, S2 and Fig. S4–S6). Compared to measurements at 298 K, both complexes exhibited a red shift in their emission maxima (6–9 nm), significantly enhanced luminescence intensity, and longer emission lifetime at 77 K. It is reasonable to consider that the emission of these complexes originates from a metal–halide-to-ligand charge transfer (MXLCT) state. The HOMO of luminescent Cu(I) complexes is often mainly localized on the Cu–I cluster, while the LUMO is frequently localized on the ligands, resulting in a small overlap between the HOMO and LUMO.[5,6] Consequently, the energy gap between the singlet and triplet states (ΔE_{ST}) becomes relatively small, which provides favourable conditions for the occurrence of TADF (thermally activated delayed fluorescence).[20] These results indicate that the emission mechanism is delayed fluorescence dominant at 298 K,[21] while phosphorescence is the predominant pathway at 77 K. Based on the spectroscopic data, ΔE_{ST} can be estimated to be approximately 0.05 eV, which is consistent with the TADF mechanism.

The two emissions of **$Cu_4I_4(L1)_2$·2CH_3CN** observed at 77 K (Fig. S6(a), 502 nm and 517 nm) are attributable to the vibronic structure of $T_1 \rightarrow S_0$ (0–0 and 0–1). The energy difference of the two emission peaks (502 nm and 517 nm) is *ca.* 578 cm^{-1}, which corresponds to the stretching vibration of the Cu–N≡C–CH_3 moiety at approximately 400–600 cm^{-1}. The two peaks share the same excitation spectra (Fig. S6(a), 417 nm) and exhibit almost identical lifetimes within experimental error (Fig. S5(b), λ_{em}: 502 nm: τ = 28.90 ± 0.74 μs and λ_{em}: 517 nm: τ = 28.70 ± 0.70 μs). The results strongly suggest that they represent vibronic sidebands of a single excited state rather than two distinct emissive states. Furthermore, the absence of a resolved vibrational structure in the **$Cu_4I_4(L1)_2$** complex can be attributed to the lack of coordinated acetonitrile, which prevents the vibrational modes associated with the Cu–N≡C–CH_3 moiety.

Conflicts of interest

The authors declare no competing financial interest.

Data availability

The data supporting this article have been included as part of the supplementary information (SI). Supplementary information is available: experimental section, crystal packing diagram, TGA, PXRD, emission lifetime measurement, excitation spectra and emission spectra. See DOI: https://doi.org/10.1039/d5dt01893e.

CCDC 2477874 contains the supplementary crystallographic data for this paper.[22]

Acknowledgements

This work was financially supported by a Grant-in-Aid for Scientific Research (C) (no. JP25K08585) from the Ministry of Education, Culture, Sports, Science, and Technology, Japan. This work was also performed in part under the Cooperative Research Program of Network Joint Research Centre for Materials and Devices (no. 20251109).

References

1 (*a*) A. C. Grimsdale, K. L. Chan, R. E. Martin, P. G. Jokisz and A. B. Holmes, *Chem. Rev.*, 2009, **109**, 897–1091; (*b*) L. Basabe-Desmonts, D. N. Reinhoudt and M. Crego-Calama, *Chem. Soc. Rev.*, 2007, **36**, 993–1017; (*c*) Z. Yang, J. Cao, Y. He, J. H. Yang, T. Kim, X. Peng and J. S. Kim, *Chem. Soc. Rev.*, 2014, **43**, 4563–4601; (*d*) M. Zhu and C. Yang, *Chem. Soc. Rev.*, 2013, **42**, 4963–4976.

2 (*a*) A. Kobayashi and M. Kato, *Chem. Lett.*, 2017, **46**, 154–162; (*b*) M. Kato, H. Ito, M. Hasegawa and K. Ishii, *Chem. – Eur. J.*, 2019, **25**, 5105–5112; (*c*) P. Naumov, S. Chizhik, M. K. Panda, N. K. Nath and E. Boldyreva, *Chem. Rev.*, 2015, **115**, 12440–12490; (*d*) *Soft Crystals: Flexible Response Systems with High Structural Order*, ed. M. Kato and K. Ishii, Springer, Singapore, 2023.

3 (*a*) D. Volz, M. Wallesch, C. Fléchon, M. Danz, A. Verma, J. M. Navarro, D. M. Zink, S. Bräse and T. Baumann, *Green Chem.*, 2015, **17**, 1988–2011; (*b*) P. C. Ford, E. Cariati and J. L. Bourassa, *Chem. Rev.*, 1999, **99**, 3625–3648; (*c*) M. Vitale and P. C. Ford, *Coord. Chem. Rev.*, 2001, **219–221**, 3–16; (*d*) A. Barbieri, G. Accorsi and N. Armaroli, *Chem. Commun.*, 2008, 2185–2193; (*e*) E. Cariati, E. Lucenti, C. Botta, U. Giovanella, D. Marinotto and S. Righetto, *Coord. Chem. Rev.*, 2016, **306**, 566–614; (*f*) P. C. Ford, *Coord. Chem. Rev.*, 1994, **132**, 129–140; (*g*) R. Peng, M. Li and D. Li, *Coord. Chem. Rev.*, 2010, **254**, 1–18; (*h*) K. Tsuge, Y. Chishina, H. Hashiguchi, Y. Sasaki, M. Kato, S. Ishizaka and N. Kitamura, *Coord. Chem. Rev.*, 2016, **306**, 636–651; (*i*) A. Mensah, J.-J. Shao, J.-J. Ni, G.-J. Li, F.-M. Wang and L.-Z. Chen, *Front. Chem.*, 2022, **9**, 816363; (*j*) J. Beaudelot, S. Oger, S. Peruško, T.-A. Phan, T. Teunens, C. Moucheron and G. Evano, *Chem. Rev.*, 2022, **122**, 16365–16609; (*k*) Y. Liu, S.-C. Yiu, C.-L. Ho and W.-Y. Wong, *Coord. Chem. Rev.*, 2018, **375**, 514–557; (*l*) V. W.-W. Yam, V. K.-M. Au and S. Y.-L. Leung, *Chem. Rev.*, 2015, **115**, 7589–7728.

4 (*a*) Y. Yamanoi, *Acc. Chem. Res.*, 2023, **56**, 3325–3341; (*b*) Y. Yamanoi, *Phys. Chem. Chem. Phys.*, 2025, **27**, 14517–14525.

5 (*a*) T. Nakae, M. Nishio, T. Yamada and Y. Yamanoi, *Molecules*, 2021, **26**, 6852; (*b*) Y. Zhao, T. Nakae, S. Takeya, M. Hattori, D. Saito, M. Kato, Y. Ohmasa, S. Sato, O. Yamamuro, T. Galica, E. Nishibori, S. Kobayashi, T. Seki, T. Yamada and Y. Yamanoi, *Chem. – Eur. J.*, 2023, **29**, e202204002.

6 Y. Zhao, T. Nakae, M. Yoshida, M. Kato, K. Omoto, S. Ito and Y. Yamanoi, *Inorg. Chem.*, 2024, **63**, 22361–22371.

7 As related studies, Hg(II) and Zn(II) complexes with 1,1,2,2-tetramethyl-1,2-dipyridin-3-yl)disilane have been reported. See: (*a*) E. Choi, H. Lee, T. H. Noh and O.-S. Jung, *CrystEngComm*, 2016, **18**, 6997–7002; (*b*) E. Choi, M. Ryu, H. Lee and O.-S. Jung, *Dalton Trans.*, 2017, **46**, 4595–4601.

8 N. Rani, G. K. Rao and A. K. Singh, *J. Organomet. Chem.*, 2009, **694**, 2442–2447.

9 (*a*) O. S. Wenger, *Chem. Rev.*, 2013, **113**, 3686–3733; (*b*) X. Zhang, B. Li, Z.-H. Chen and Z.-N. Chen, *J. Mater. Chem.*, 2012, **22**, 11427–11441; (*c*) E. Li, K. Jie, M. Liu, X. Sheng, W. Zhu and F. Huang, *Chem. Soc. Rev.*, 2020, **49**, 1517–1544; (*d*) M. Kato, M. Yoshida, Y. Sun and A. Kobayashi, *J. Photochem. Photobiol., C*, 2022, **51**, 100477; (*e*) M. Kato, Chromic behaviors and color control of luminescent copper(I) complexes, in *Photochemistry and Photophysics of Earth-Abundant Transition Metal Complexes*, ed. R. V. Eldik and P. C. Ford, Elsevier, 2024, vol. 83, pp. 33–62; (*f*) Q. Zhao, F. Li, C. Li, Z.-H. Chen and Z.-N. Chen, *Chem. Soc. Rev.*, 2010, **39**, 3007–3030; (*g*) X. Zhang, B. Li, Z.-H. Chen and Z.-N. Chen, *J. Mater. Chem.*, 2012, **22**, 11427–11441; (*h*) A. Kobayashi and M. Kato, *Eur. J. Inorg. Chem.*, 2014, 4469–4483.

10 T. Hasegawa, A. Kobayashi, H. Ohara, M. Yoshida and M. Kato, *Inorg. Chem.*, 2017, **56**, 4928–4936.

11 S. Kondo, N. Yoshimura, A. Kobayashi, K. D. C. Kuruppu, W. M. C. Sameera, S. Fujii, M. Yoshida and M. Kato, *J. Mater. Chem. C*, 2024, **12**, 1799–1808.

12 (*a*) W.-F. Fu, X. Gan, C.-M. Che, Q.-Y. Cao, Z.-Y. Zhou and N.-Y. Zhu, *Chem. – Eur. J.*, 2004, **10**, 2228–2236; (*b*) A. Kobayashi, K. Komatsu, H. Ohara, W. Kamada, Y. Chishina, K. Tsuge, H.-C. Chang and M. Kato, *Inorg. Chem.*, 2013, **52**, 13188–13198; (*c*) S. Ito, K. Tanaka and Y. Chujo, *Dalton Trans.*, 2025, **54**, 9219–9225.

13 K. Sato, M. Hattori and Y. Yamanoi, *RSC Adv.*, 2025, **15**, 16968–16972.

14 E. R. Barth, C. Golz, M. Knorr and C. Strohmann, *Acta Crystallogr., Sect. E:Crystallogr. Commun.*, 2015, **71**, m189–m190.

15 (*a*) B. Cordero, V. Gómez, A. E. Platero-Prats, M. Revés, J. Echeverría, E. Cremades, F. Barragán and S. Alvarez, *Dalton Trans.*, 2008, 2832–2838; (*b*) A. Bondi, *J. Phys. Chem.*, 1964, **68**, 441–451.

16 (*a*) L. Garzón-Tovar, Á. Duarte-Ruiz and K. Wurst, *Inorg. Chem. Commun.*, 2013, **32**, 64–67; (*b*) K.-T. Youm, J. Ko and M.-J. Jun, *Polyhedron*, 2006, **25**, 2717–2720.

17 (*a*) N. T. Kim, H. Li, L. Venkataraman and J. L. Leighton, *J. Am. Chem. Soc.*, 2016, **138**, 11505–11508; (*b*) P. Gualco, S. Ladeira, K. Miqueu, A. Amgoune and D. Bourissou, *Angew. Chem., Int. Ed.*, 2011, **50**, 8320–8324; (*c*) P. Gualco, S. Ladeira, K. Miqueu, A. Amgoune and D. Bourissou, *Organometallics*, 2012, **31**, 6001–6004; (*d*) P. Gualco, A. Amgoune, K. Miqueu, S. Ladeira and D. Bourissou, *J. Am. Chem. Soc.*, 2011, **133**, 4257–4259.

18 (*a*) P. Kar, M. Yoshida, Y. Shigeta, A. Usui, A. Kobayashi, T. Minamidate, N. Matsunaga and M. Kato, *Angew. Chem., Int. Ed.*, 2017, **56**, 2345–2349; (*b*) E. J. Fernández, J. M. López-de-Luzuriaga, M. Monge, M. E. Olmos, R. C. Puelles, A. Laguna, A. A. Mohamed and J. P. Fackler, *Inorg. Chem.*, 2008, **47**, 8069–8076; (*c*) J. Vallejo, E. Pardo, M. V. Chumillas, I. Castro, P. Amoros, M. Deniz, C. Ruiz-Perez, C. Y. Vivas, J. Krzystek, M. Julve, F. Lloret and J. Cano, *Chem. Sci.*, 2017, **8**, 3694–3702.

19 D. E. Royzman, A. M. Noviello, K. M. Henline, R. D. Pike, J. P. Killarney, H. H. Patterson, C. Crawford and Z. Assefa, *J. Inorg. Organomet. Polym.*, 2014, **24**, 66–77.

20 (*a*) R. Ishimatsu, S. Matsunami, T. Kasahara, J. Mizuno, T. Edura, C. Adachi, K. Nakano and T. Imato, *Angew. Chem., Int. Ed.*, 2014, **53**, 6993–6996; (*b*) H. Tanaka, K. Shizu, H. Miyazaki and C. Adachi, *Chem. Commun.*, 2012, **48**, 11392–11394.

21 For the examples on metal complexes showing TADF, see: (*a*) E. Cariati, D. Roberto, R. Ugo, P. C. Ford, S. Galli and A. Siron, *Inorg. Chem.*, 2005, **44**, 4077–4085; (*b*) H. V. R. Dias, H. V. K. Diyabalanage, M. G. Eldabaja, O. Elbjeirami, M. A. Rawashdeh-Omary and M. A. Omary, *J. Am. Chem. Soc.*, 2005, **127**, 7489–7501; (*c*) A. Kobayashi, T. Ehara, M. Yoshida and M. Kato, *Inorg. Chem.*, 2020, **59**, 9511–9520; (*d*) L. Kang, J. Chen, T. Teng, X.-L. Chen, R. Yu and C.-Z. Lu, *Dalton Trans.*, 2015, **44**, 11649–11659.

22 CCDC 2477874: Experimental Crystal Structure Determination, 2025, DOI: 10.5517/ccdc.csd.cc2p5ffr.